# The Influence of Sea-Surface Temperature on Surface Wind in the Eastern Equatorial Pacific: Seasonal and Interannual Variability

J. M. WALLACE, T. P. MITCHELL AND C. DESER

*Department of Atmospheric Sciences, University of Washington, Seattle, Washington*

(Manuscript received 27 February 1989, in final form 3 August 1989)

ABSTRACT

The climate of the eastern Pacific exhibits a pronounced equatorial asymmetry. Boundary layer air originating in the Southern Hemisphere trades crosses the equator and flows into the intertropical convergence zone (ITCZ), whose southern limit is nearly always located at least 4° to the north of the equator. The sea-surface temperature (SST) distribution is characterized by a prominent "cold tongue" centered ~1°S, a strong frontal zone centered ~2°N, and a warm eastward current centered near 5°N. The surface wind field exhibits a pronounced horizontal divergence as the air flows northward across the oceanic frontal zone.

These features vary in strength in response to the annual cycle and the El Niño/Southern Oscillation phenomenon. The northward cross-equatorial surface winds, the cold tongue and the frontal zone all tend to be strongest during the cold season (July through November). During the cold season of the coldest years, when the cold tongue is most prominent, the cross-equatorial flow tends to be weaker than normal and the northward flow across 5°N stronger than normal.

It is shown that within a few degrees of the equator the meridional equation of motion for the surface winds reduces to a balance between the pressure gradient force and the frictional term that involves the vertical derivative of the vertical flux of momentum by subgrid scale processes. Some of the seasonal and interannual variability of the surface winds appears to be a response to the hydrostatic sea-level pressure changes induced by variations in the strength of the cold tongue. However, that the maximum divergence of the surface winds is observed directly above the oceanic frontal zone rather than over the cold tongue appears to be due to the reduction in vertical wind shear within the lowest 100 m that occurs as air parcels pass northward from the cold tongue to the much warmer waters of the North Equatorial Countercurrent. As evidence of the existence of strong vertical wind shear in the stable boundary layer regime over the cold tongue, we note that northward velocities just 100 m above sea level at the Galapagos Islands have been reported to be on the order of 15 m $s^{-1}$; more than twice as strong as the surface winds.

## 1. Introduction

The surface winds in the equatorial Pacific east of 120°W nearly always exhibit a strong southerly component, a feature that has not been well simulated in general circulation models and has been not been well handled by the various data assimilation systems used in operational numerical weather prediction (e.g., see Reynolds et al. 1989). The southeasterly trades cross the equator and feed into the intertropical convergence zone (ITCZ), which is almost always situated over the northern tropics, as shown in Fig. 1. The northward flow appears to be largely confined to the layer below 1 km (Hastenrath 1977). The distribution of sea-surface temperature (SST), also shown in Fig. 1, exhibits a prominent equatorial "cold tongue" centered along ~1°S and a strong frontal zone extending from the equator to ~5°N.

*Corresponding author address:* Prof. John M. Wallace, Dept. of Atmospheric Sciences, AK-40, University of Washington, Seattle, WA 98195.



The cold tongue and the frontal zone are nearly always present but their strength varies both seasonally and on the interannual time scale. The seasonal cycle in this region follows the Southern Hemisphere, but it is delayed by a month or two (Sadler 1987). The "cold season" extends from July through November, and the somewhat shorter "warm season" from March through May. The southerly flow across the equator is almost twice as strong during the cold season as during the warm season; the cold tongue is more prominent, and the ITCZ is located farther northward.

The interannual variability in this region is dominated by the El Niño/Southern Oscillation (ENSO) phenomenon, which is clearly defined during the cold season. The Rasmusson and Carpenter (1982) warm event composite for the "transition phase" (August through October) of a typical warm year is characterized by stronger than normal southerly flow across the equator, a weakening of the cold tongue, and a southward displacement of the ITCZ. The same features are apparent in regressions of surface winds upon indices of Darwin sea-level pressure (Wright et al. 1988). Hence the interannual variability associated with the

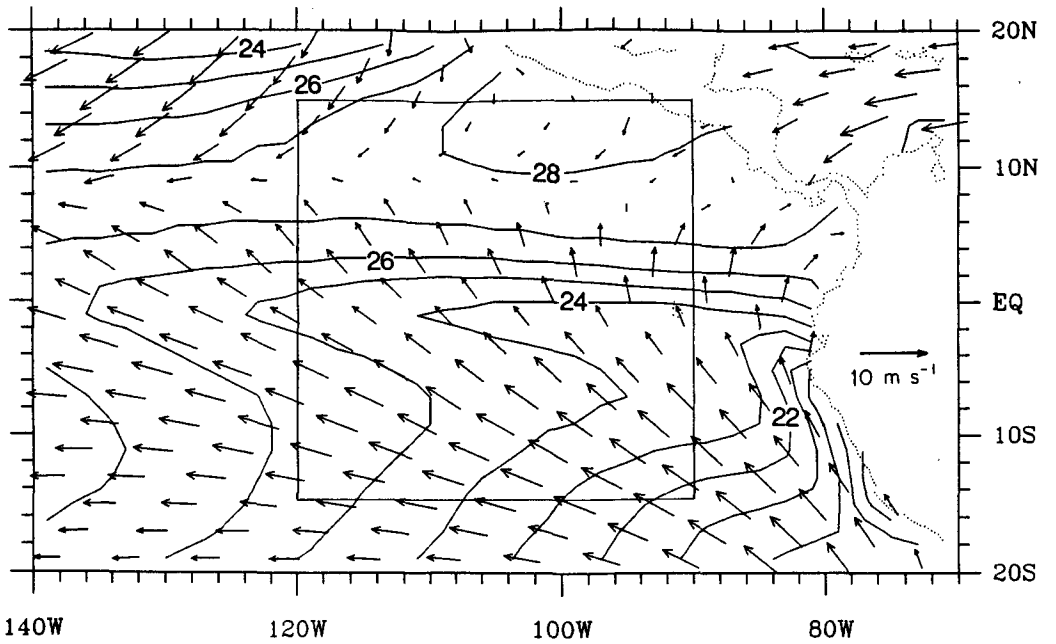


FIG. 1. Annual average SST and surface wind over the eastern Pacific, based upon the atlas of Sadler et al. (1987). Contour interval 1°C. The rectangle represents the domain of the meridional profiles in Figs. 2–4.

ENSO phenomenon in this region has its own distinctive signature: it cannot be viewed simply as a modulation of the climatological mean annual cycle.

Our efforts to understand these subtle but systematic differences between the annual cycle and the interannual variability in the structure of the meridional wind field over the eastern Pacific have yielded some useful insights into the cross-equatorial flow in the atmospheric planetary boundary layer, its interaction with the equatorial cold tongue, and its role in producing an ITCZ whose sharply defined southern edge is nearly always located at least a few degrees north of the equator. In a related paper (in this issue) Hayes et al. (1989) have shown that the same dynamical processes are evident in the day-to-day variability in this region.

## 2. Data and analysis procedures

Most of the results presented in this paper are based on monthly mean grids of sea-surface temperature (SST), sea-level pressure ($p$), meridional wind component ($v$), sea-air temperature differences, and relative humidity for the period 1946–85, extracted from the Comprehensive Ocean/Atmosphere Data Set (COADS), obtained from the NCAR Data Library. Climatological mean statistics representing conditions during the cold season (July–November) and warm season (March–May) are based on Sadler et al.'s (1987) analysis of the COADS. We will also compare statistics based on composite charts for the cold season of "warm years" and "cold years" observed in association with the ENSO phenomenon. The procedures used in constructing these composite charts are justified by documentary evidence presented in Wright et al. (1988) to the effect that linear correlations between these variables during the cold season are very strong, and our unpublished results which indicate that anomaly patterns for warm and cold years are very similar, apart from the reversal in polarity. We will take account of the fact that the anomalies in these variables observed during warm years are, on average, almost twice as large as those observed during cold years. Our composite charts are constructed by regressing the fields of each of the three variables upon an index of equatorial Pacific SST, $T_E$ (defined as cold season SST anomaly averaged from 6°N–6°S, from the date line to the South American coast). For the meridional wind component, $v$, composite values for the cold and warm years are given by

$$v_c = \bar{v} + T_c \frac{\sum v_i'(T_E)_i'}{\sum (T_E)_i'^2}, \quad v_w = \bar{v} + T_w \frac{\sum v_i'(T_E)_i'}{\sum (T_E)_i'^2}$$

respectively, where overbars $\overline{(\ )}$ and primes $(\ )'$ denote means and anomalies from the Sadler et al. climatology, respectively; $i$ refers to the cold season for a particular calendar year; the summations are over the 40 cold seasons (1946–85); and $T_c$ and $T_w$ are typical values of $T_E$ anomalies during the cold seasons of cold and warm years of the ENSO cycle. For $T_c$ and $T_w$, we used values of −0.8° and 1.4°C, which represent the average values of $T_E$ during the five coldest and five warmest July–November seasons of the record (1946–85), respectively. $T_E$ exceeded 1.4°C during 1972 and

1982 and it was below −0.8°C during 1954, 1955, and 1970. Analogous regression equations were used for the other variables.

All meridional profiles shown in section 3 are based upon data that were averaged zonally within the sector 90°–120°W, as indicated by the rectangle in Fig. 1. The data are available at 2° latitude intervals centered on ±1°, ±3°, etc.

## 3. Results

Figure 2 shows meridional profiles of warm minus cold season difference ($\Delta$) in sea-surface temperature (SST), sea-level pressure ($p$), and meridional wind component ($v$), and Fig. 3 shows meridional profiles of warm minus cold year differences ($\delta$) in the same variables, based on composites for the warm and cold seasons. Consistent with the foregoing discussion, the northward flow across the equator is stronger during the cold season than during the warm season, but it tends to be stronger during the cold seasons of warm years than during the cold seasons of cold years. The correlation coefficient between $v$ at 1°S and $T_E$ averaged for the cold season based on data for 1946–85 [hereafter denoted as $r(v, T_E)$] is +0.78: hence the latter relationship is a rather dependable one. It is evident from Fig. 3 that the relationship between $v$ and $T_E$ is strongly latitude dependent; e.g., poleward of 4°N and 9°S the northward flow tends to be stronger during cold years than during warm years.

From a comparison of Figs. 2 and 3 it is evident that the seasonal and interannual variability of SST tends to be largest in the climatological mean cold tongue centered at 1°S. The interannual variability is more concentrated in the latitude belt of the cold tongue than the seasonal variability. Within the equatorial belt sea-level pressure is negatively correlated with $T_E$ in both the seasonal and interannual variability:

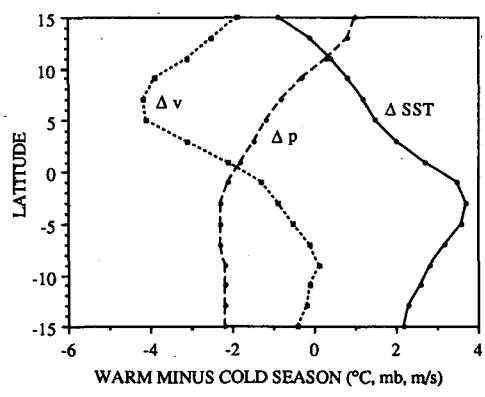


FIG. 2. Warm season (March–May) minus cold season (July–November) meridional profiles of sea-surface temperature, sea-level pressure, and the meridional component of the surface wind, based upon the atlas of Sadler et al. (1987). Expressed in units of degrees Celsius, millibars, and meters per second.

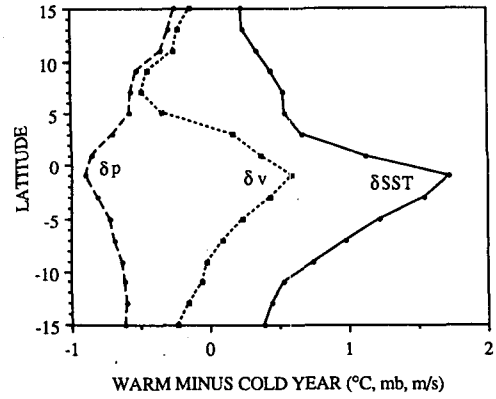


FIG. 3. Warm year minus cold year meridional profiles of sea-surface temperature, sea-level pressure, and the meridional component of the surface wind during the cold season, in units of degrees Celsius, millibars, and meters per second, during the period 1946–85. See text for definition of warm and cold years.

$r(p, T_E) \leq -0.8$ from 10°N–10°S. However, the meridional profiles of the pressure anomalies are broader than those of the SST anomalies. Hence, if the pressure anomalies are a hydrostatic, planetary boundary layer response to the SST anomalies, it is evident that processes within the atmosphere must be acting to spread out the pressure perturbations in the meridional direction. In Fig. 2 the broad negative peak in $\Delta v$ centered near 7°N coincides with a maximum seasonal contrast in the meridional pressure gradient $\partial/\partial y(\Delta p)$, whereas in Fig. 3 the positive maximum in $\delta v$ at 1°S coincides with a local extremum in $\delta p$, where $\partial/\partial y(\delta p) \sim 0$.

It is possible to gain some insight into the meridional structures of the $\Delta v$ and $\delta v$ profiles by considering meridional profiles of SST, $p$ and $v$ during the warm season and typical profiles of the same variables representative of the cold seasons of warm and cold years, as shown in Fig. 4.

The SST profiles in the left panel show that the equatorial cold tongue, a well-known feature of the climatology, is usually present throughout the year. It is enhanced during cold years, and it just about disappears during the warmest years. The meridional SST gradient between the equator and 5°N varies by about a factor of three between the warm and cold years.

Sea-level pressure, shown in the middle panel, exhibits a much stronger meridional gradient during the cold season than during the warm season. Even in the presence of the cold tongue, $p$ decreases monotonically from south to north during a typical cold season. During the warm years the stronger meridional pressure gradients are observed to the south of the cold tongue, whereas during the cold years they are observed to the north of the cold tongue. These differences reflect, to some degree, the denser air in the planetary boundary layer over the cold tongue during the cold years.

The meridional wind component shown in the right-

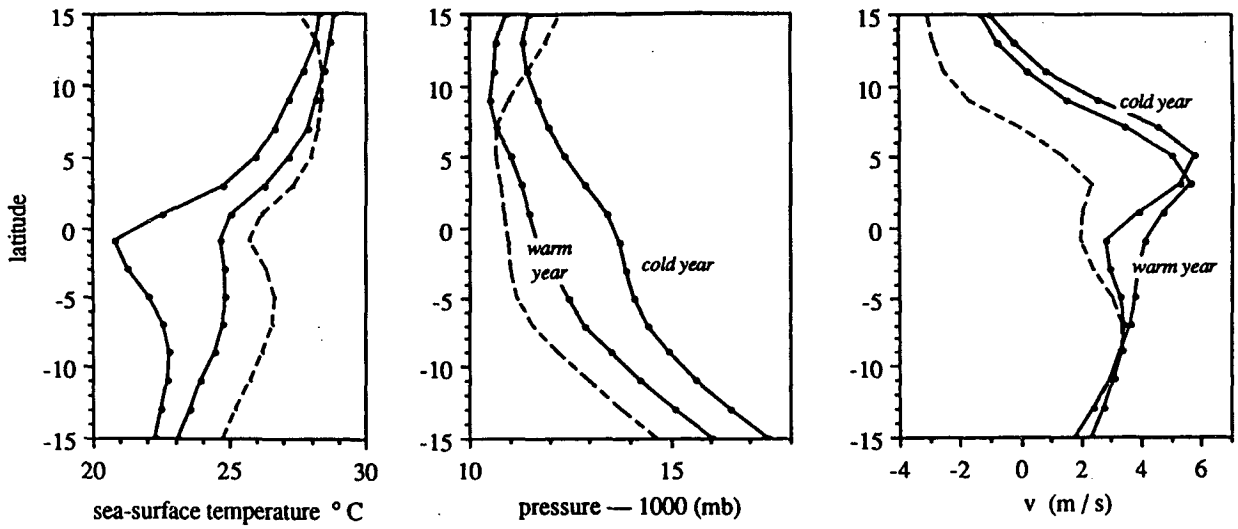


FIG. 4. Meridional profiles of (a) SST, (b) sea-level pressure, and (c) the meridional wind component for the climatological mean warm season (dashed) and the cold seasons of the warm and cold years (solid). See text for definition of warm and cold years.

hand panel tends to be stronger during the cold season, particularly in the northern tropics, where it approaches values of 6 m $s^{-1}$ near 5°N. This wind maximum has been noted previously by Hastenrath (1977), who pointed out that it marks the boundary between a narrow band of rather strong divergence in the surface wind field, centered about 2°N, and the ITCZ farther to the north. During the warm years the strength of the southerly flow increases monotonically from the Southern Hemisphere subtropics to a single maximum at 3°–4°N, whereas during the cold years air parcels decelerate as they approach the cold tongue from the south and then accelerate sharply as they cross the oceanic frontal zone from the equator to 5°N, with horizontal divergences on the order of $5 \times 10^{-6}$ $s^{-1}$.

## 4. Discussion

In our efforts to understand why the meridional profile of $v$ is so different from that of the meridional pressure gradient, we considered the leading terms in the time-averaged horizontal momentum equation for the surface winds in this region in the form

$$-\frac{\partial \Phi}{\partial y} - v\frac{\partial v}{\partial y} - fu = -\frac{\partial}{\partial z}\left(\frac{\tau_y}{\rho}\right) \qquad (1)$$

where $\Phi$ is geopotential in units of $m^2$ $s^{-2}$ $\approx$ [($p$ − 1000 mb) × 80], $\tau_y$ the upward flux of northward momentum by subgrid scale motions, and the other symbols have their conventional meanings. In view of the small zonal gradients in Fig. 1, we have neglected the zonal advection of momentum. For the surface momentum balance, we should also be justified in neglecting the vertical advection. S. L. Hayes (personal communication) calculated the contribution of the transient wind fluctuations within a 5-month cold season to the meridional advection of momentum, using daily surface wind data from Atlas moorings along the 110°W meridian at 2°N, on the equator, and at 2°S, and found it to be an order of magnitude smaller than the advection by the time mean flow. So we believe that (1) should contain all the potentially important terms in the meridional momentum balance at the earth's surface within the region of interest.

The nonlinear advection term $-v\partial u/\partial y$ is of first-order importance in the zonal equation of motion in the equatorial belt in regions of cross-equatorial flow such as the western Indian Ocean, where the eastward directed pressure gradient force tends to be in cyclostrophic balance with the centripetal acceleration of the flow (Stout and Young 1983; Young 1987). From an inspection of Fig. 4c it is evident that its counterpart $-v\partial v/\partial y$ in (1) should be strong over the oceanic frontal zone, near 2°N, where it should tend to oppose the northward directed pressure gradient force. However, it is readily verified that it is only about one-fifth as large as $-\partial\Phi/\partial y$ in that region. Hastenrath and Lamb (1978) also concluded that the advection term is of secondary importance in their analysis of marine surface observations over the eastern Pacific (80°–100°W). Given the westward component of the low-level flow over this region, the $-fu$ term must contribute to an equatorial divergence of the surface winds through the action of the $\beta$ effect. However, it is evident from Fig. 1 that the easterlies are largely confined to the western half of the domain of interest and even there they are not as large as over the region westward of 120°W.

We have examined the meridional profile of the sum of the three terms on the left-hand side of (1) (not shown here) and found it to be very similar to the profile of $-\partial\Phi/\partial y$ alone, at least within 5° of the equa-

tor. Hence, to first order, the pressure gradient force must be balanced by the stress term on the right-hand side. The latter may be viewed as consisting of a linear component, proportional to the surface wind, which acts as a drag force, and a nonlinear component, which varies spatially in response to changes in the vertical wind profile and the intensity of the vertical mixing by motions within the boundary layer. If the linear component were dominant, we should expect that the strongest northward wind speeds would coincide with the strongest southward directed pressure gradients. Since this is clearly not the case, nonlinear effects must be important. We will now consider the processes that might be important.

As the air in the planetary boundary layer flows northward from the southern trades towards the equatorial cold tongue it becomes stably stratified, as evidenced by the fact that during the cold seasons of the cold years surface air temperatures at these latitudes are warmer than the underlying sea-surface temperatures by more than 0.3 K (Fig. 5a); more than enough to offset the destabilizing influence of the virtual temperature effect. (During the cold seasons of the warm years air temperatures over the cold tongue are just about the same as the sea-surface temperatures.) Rawinsonde data for Guayaquil (3°S), shown in Table 1, indicate that during the cold seasons of non El Niño years, the planetary boundary layer is stably stratified down to below 950 mb, and the lapse rate averaged over the lowest kilometer is less than 5° K km$^{-1}$. Under these conditions it is reasonable to expect the surface winds to be relatively decoupled from the strong northward flow aloft. Suppression of the vertical mixing by the high static stability would explain not only the minimum in southerly wind speed, but also the maximum in the relative humidity of the surface air over the cold tongue (Fig. 5b). It would also explain why wind speeds tend to be lightest and relative humidities highest during cold seasons of the cold years, when the cold tongue is most pronounced. The tendency for light surface winds over the cold tongue is also evident in the maps of the northward component of the surface wind velocity during the cold season (shown in Fig. 6). Enfield (1981) invoked a similar mechanism to explain the increase in relative humidity during cold years along the coastal upwelling zone off Peru.

As air parcels cross the oceanic frontal zone toward the warmer waters of the North Equatorial Countercurrent, the atmospheric boundary layer undergoes a transition from a stable to an unstable regime, as evidenced by the sea–air temperature differences in excess of 1 K in Fig. 5a. Such a transition should favor an increase in the surface wind speed through the enhanced downward flux of northward momentum from aloft by the increasingly vigorous, buoyancy-driven turbulence. It should also favor a decrease in relative humidity of the surface air due to the enhanced downward mixing of drier air from aloft. It is evident from Fig. 5b that relative humidity does, in fact, drop by ~5% as the air crosses the oceanic frontal zone during the cold season of the cold years.

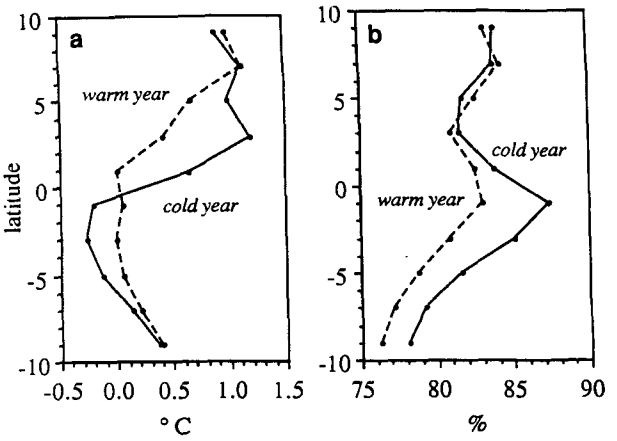


FIG. 5. Meridional profiles of (a) sea–air temperature difference, and (b) relative humidity for the cold seasons of the warm and cold years. See text for definition of warm and cold years.

TABLE 1. Guayaquil temperature (°C), July–September averages: 1957 was an El Niño year and 1960 a normal year.

| | 1957 | 1960 |
|---|---|---|
| Surface | 24.9 | 21.2 |
| 950 mb | 21.1 | 17.9 |
| 900 mb | 18.8 | 17.9 |
| 850 mb | 16.0 | 15.8 |
| 800 mb | 14.6 | 14.8 |

Table 2 shows climatological mean data for the Galapagos station[1], which provide an indication of the winds aloft over the cold tongue. During the cold season the northward wind component reported at the 1000 mb level (~110 m above sea level) is, on average, more than twice as strong as the reported surface wind. This strong vertical shear is further evidence of the strong boundary layer stratification that prevails over the cold tongue. During three of the four years of the record the southerly wind speeds reported at the 1000 mb level approach values of 15 m s$^{-1}$: strong enough to justify the label *low-level jet*. As noted previously by Hastenrath (1977), the southerly flow is largely confined to the lowest kilometer of the atmosphere and the wind maximum appears to be located much closer to the earth's surface than to the top of the planetary boundary layer.

[1] Based on unpublished data for 1967–71 supplied to S. Hastenrath (University of Wisconsin) by the Instituto Nacional de Meteorologia y Hydrologia of Ecuador and kindly made available to us by Professor Hastenrath. Unfortunately, we do not know how the raw data were processed to obtain the reported 1000 mb wind, but we presume that these observations refer to vertical averages over the lowest few hundred meters of the soundings. These results need to be verified.

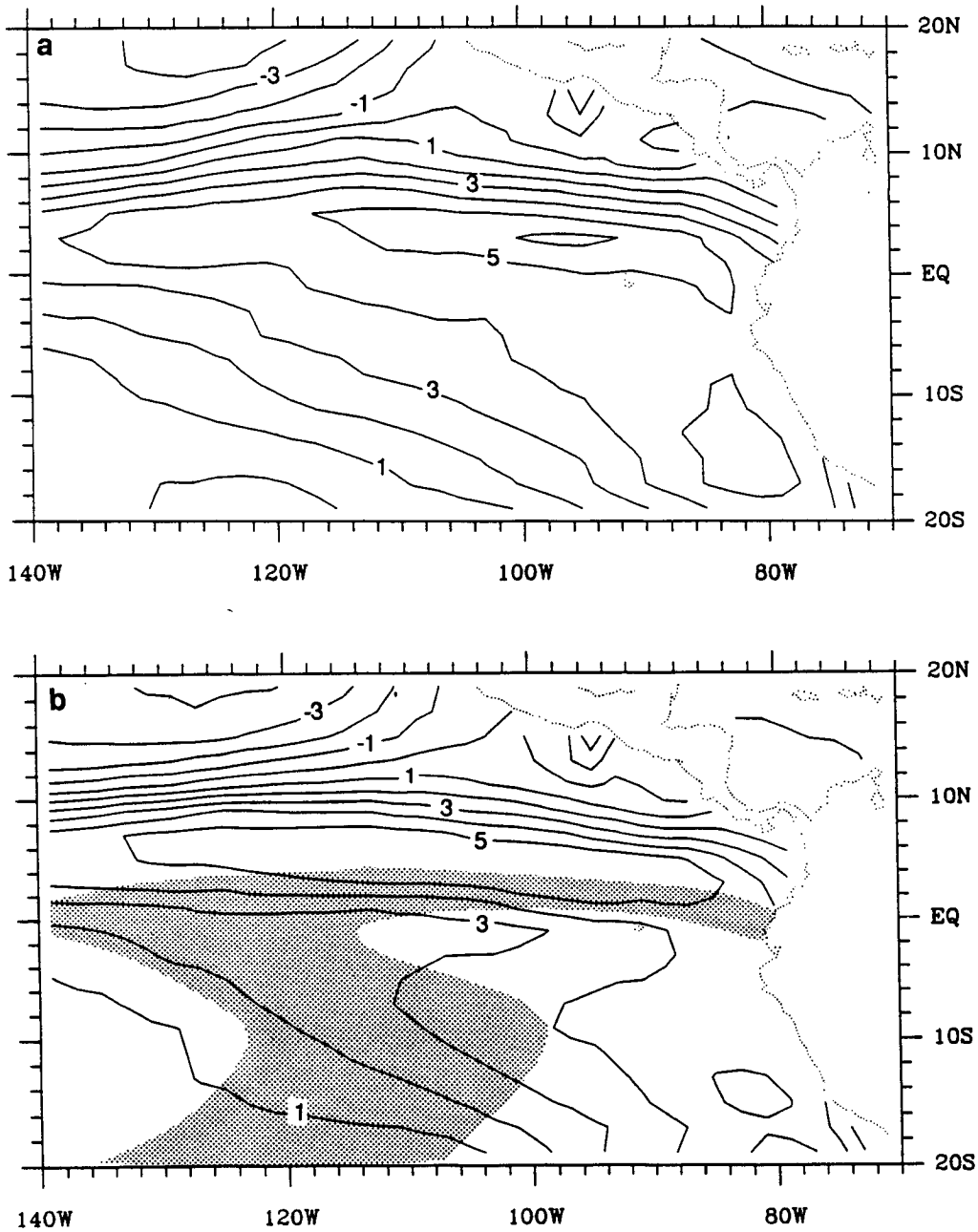


FIG. 6. Magnitude of the meridional wind component during the cold seasons of (a) the warm years, and (b) the cold years. Contour interval 1 m $s^{-1}$. Shading in (b) denotes sea-surface temperatures between 22° and 25°C, which delineate the oceanic frontal zone.

We suspect that the wind profile might change substantially as the air flows northward over the oceanic frontal zone and the boundary layer becomes destabilized. The strong, northward directed pressure gradient force observed at the earth's surface over the frontal zone should extend upward at least partway through the planetary boundary layer, accelerating the winds aloft. As the boundary layer flow crosses the zone it is also subject to an increasing wind stress at the air–sea interface, as inferred from the marked increase in surface wind speed. Horizontal divergences of the surface wind on the order of $5 \times 10^{-6}$ $s^{-1}$ are indicative of subsidence aloft, which might be large enough to produce substantial vertical advection of momentum and potential temperature. We can obtain some indication of how the winds aloft might be responding to these multiple influences by comparing soundings taken at 1.5°S and 3.0°N along 110°W by the NOAA

P-3 research aircraft on the same day during the cold season of a normal year shown in Fig. 7. The temperature and dewpoint profiles at both locations exhibit typical tropical boundary layer characteristics: a subcloud layer below ~600 m and an inversion (isothermal layer at 3°N) marked by a sharp decrease in humidity with height from 1400 to 1600 m, which marks the top of the planetary boundary layer. In both profiles, the southerly flow is largely confined to the planetary boundary layer. At 1.5°S, the strongest vertical wind shear appears to be confined to the layer below ~150 m: the easterly flow 100 m above the sea surface is ~13 m $s^{-1}$, more than 3 times as strong as the climatological mean easterlies at the surface as deduced from COADS, and the southerly flow is twice as strong as at the surface. In contrast, the wind shear at 3°N appears to be fairly uniformly distributed through the lowest 600 m. Admittedly, these wind profiles are only instantaneous samples, but they support the notion that the wind shear is stronger and confined to a thinner layer over the cold tongue than over the frontal zone.

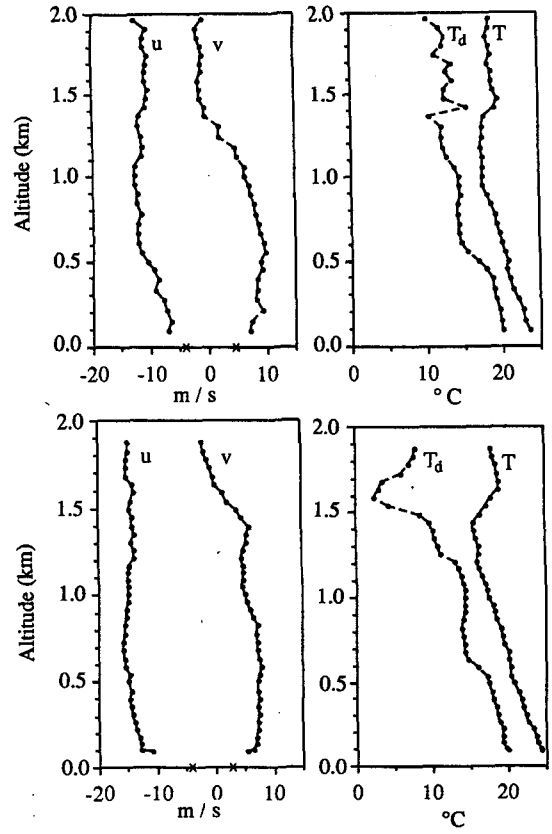


FIG. 7. Soundings taken at 3.0°N (upper panel) and 1.5°S (lower panel) along 110°W by the NOAA P-3 research aircraft on 2 July 1979 at around noon local time, courtesy of Dr. Gary Greenhut (Climate Research Division, Air Resources Laboratory, NOAA/CIRES). The lowest aircraft measurement is at 90 m. The crosses denote the climatological mean values of surface wind based on COADS. Profiles for the zonal and meridional wind components are in the left-hand panels and temperature and dewpoint are in the right-hand panels.

## 5. Concluding remarks

Lindzen and Nigam (1987) have argued that much of the observed horizontal structure in the boundary layer wind field is driven by horizontal pressure gradients that develop in response to the boundary layer baroclinity induced by the underlying SST gradients. In agreement with results based on their simple boundary layer formulation, we find that in the eastern equatorial Pacific the surface winds tend to blow consistently across the isobars from higher toward lower pressure and across the isotherms from colder toward warmer SST. Consistent with their notion of a "back pressure effect," which has the effect of smoothing out the pressure gradients in the equatorial zone, we find that the observed sea-level pressure gradients tend to be less concentrated than the underlying SST gradients.

In view of the secondary importance of the nonlinear advection term in (1), we had wondered whether the surface wind speeds would prove to be roughly proportional to the magnitude of the horizontal pressure gradients, as they are at higher latitudes. If this were in fact the case, the strongest southerly winds would be observed directly over the oceanic frontal zone rather than to the north of it, as shown in Fig. 6b. Spatial variations in static stability appear to be an important source of nonlinearity in this relationship.

The quasi-two-dimensionality of the planetary boundary layer flow and the remarkable strength of the underlying SST gradients render the eastern equatorial Pacific an attractive region for testing boundary layer parameterization schemes. Observations of the vertical profile of wind in the planetary boundary layer over the frontal zone would be required for testing the models. Because the phenomena of interest appear to be largely restricted to the lowest kilometer of the atmosphere and because the region of interest is relatively free of clouds, pilot balloon observations would probably be sufficient for this purpose. Moreover, because winds in this region tend to be quite steady (e.g., see Hastenrath and Lamb 1978, Fig. 1), a relatively modest number of observations should be sufficient to document the seasonal and interannual variability of the planetary boundary layer flow.

TABLE 2. Vertical-profile of the meridional wind component over San Cristobal, Galapagos Islands (0° 54'S, 89° 57'W): July–November averages in m $s^{-1}$.

| | 1967 | 1968* | 1969 | 1970 |
|---|---|---|---|---|
| Surface | 6.3 | 5.7 | 5.0 | 5.7 |
| 1000 mb | 9.9 | 14.4 | 14.0 | 13.6 |
| 900 mb | −1.0 | −0.9 | 1.0 | −0.7 |

* October data missing.

During the cold seasons of the cold years, when the meridional asymmetries are strongest, the oceanic frontal zone becomes hydrodynamically unstable, giving rise to westward propagating waves with periods on the order of a few weeks. In the companion paper by Hayes et al. (1989) it is shown that the signature of these instability waves is evident in SST and surface wind observations from an array of moored buoys at 110°W. Consistent with the boundary layer stability arguments put forth in the present paper, SST and surface wind speed exhibit a strong positive correlation on the time scale of the waves.

*Acknowledgments.* We would like to thank Drs. Stan P. Hayes, Michael P. McPhaden, and Mark Cane for their interest in this work and for their helpful comments and suggestions. This work was supported by the Climate Dynamics Program of the National Science Foundation under Grant ATM-8318853.

## REFERENCES

Enfield, D. B., 1981: Thermally driven wind variability in the planetary boundary layer above Lima, Peru. *J. Geophys. Res.*, **86**(C3), 2005–2016.

Hastenrath, S., 1977. On the upper air circulation over the equatorial Americas. *Arch. Meteor. Geophys. Bioklim. Ser. A.*, **25**, 309–321.

——, and P. Lamb, 1978. On the dynamics and climatology of the surface flow over the equatorial oceans. *Tellus*, **30**, 436–449.

Hayes, S., M. McPhaden and J. M. Wallace, 1989. The influence of sea-surface temperature upon surface wind in the eastern equatorial Pacific: Weekly to monthly variability. *J. Climate*, **2**, 1500–1506.

Lindzen, R. S., and S. Nigam, 1987. On the role of sea-surface temperature gradients in forcing low-level winds and convergence in the tropics. *J. Atmos. Sci.*, **44**, 2418–2436.

Rasmusson, E. M., and T. H. Carpenter, 1982. Variations in tropical sea-surface temperature and surface wind fields associated with the Southern Oscillation/El Niño. *Mon. Wea. Rev.*, **110**, 354–384.

Reynolds, R. W., K. Arpe, C. Gordon, S. P. Hayes, A. Leetmaa and M. J. McPhaden, 1989. A comparison of tropical Pacific surface wind analyses. *J. Climate*, **2**, 105–111.

Sadler, J. C., M. A. Lander, A. M. Hori and L. K. Oda, 1987. Tropical Marine Climatic Atlas, Vol. 2., Pacific Ocean. UHMET 87-02, University of Hawaii, Honolulu.

Stout, J. E., and J. A. Young, 1983. Low-level monsoon dynamics derived from satellite winds. *Mon. Wea. Rev.*, **111**, 774–798.

Wright, P. B., J. M. Wallace, T. P. Mitchell and C. Deser, 1988. Correlation structure of the El Niño/Southern Oscillation phenomenon. *J. Climate*, **1**, 609–625.

Young, J. A., 1987. Boundary layer dynamics of tropical and monsoonal flows. *Monsoon Meteorology*, C.-P. Chang and T. N. Krishnamurti, Eds., Oxford University Press, 540 pp.